$$(\bar{\omega}\tau)[(\bar{\omega}\tau)^3+(\bar{\omega}\tau)^2 2(1+r)+(\omega\tau)(1+4r)+2r] = (\bar{\omega}\tau)(\bar{\omega}\tau+1)^2(\bar{\omega}\tau+2r)$$

from which the double-degenerate diffusive mode at $\bar{\omega}\tau=-1$, the mode at $\bar{\omega}\tau=0$, and at $\bar{\omega}\tau=-2r$ are apparent.

*Work supported in part by funds from the National Science Foundation, under Grant No. GU-3186.

†Present address: Institut Laue-Langevin, Cedex No. 156, 38 Grenoble-Gare, France.

[1]T. M. McNelly, S. J. Rogers, D. J. Channin, R. J. Rollefson, W. M. Goubau, G. E. Schmid, J. A. Krumhansl, and R. O. Pohl, Phys. Rev. Letters 24, 100 (1970); H. E. Jackson, C. T. Walker, and T. F. McNelly, *ibid.* 25, 26 (1970).

[2]B. Taylor, H. J. Maris, and C. Elbaum, Phys. Rev. Letters 23, 416 (1969).

[3]R. A. Guyer and J. A. Krumhansl, Phys. Rev. 148, 778 (1966); 148, 766 (1966); L. Sham, *ibid.* 163, 401 (1967); 156, 494 (1967); W. Götze and K. H. Michel, *ibid.* 156, 738 (1967); 148, 766 (1967); J. Ranninger, J. Phys. C 2, 640 (1969).

[4]R. E. Peierls, Ann. Physik 3, 1055 (1929).

[5]J. A. Süssmann and A. Thellung, Proc. Phys. Soc. (London) 81, 1122 (1963).

[6]D. N. Zubarev, Fortschr. Physik 9, 275 (1961).

[7]J. Callaway, Phys. Rev. 113, 1046 (1959).

[8]To take into account the fact that phonon branches are not strictly Debye-like also leads to a temperature dependence of the second-sound velocity. Numerical evaluation of this temperature dependence by R. J. Hardy and S. S. Jaswal [Phys. Rev. 3, 1440 (1971)] for NaF and B. J. Bennett [Solid State Commun. 8, 65 (1970)] for rare-gas solids show also a decrease in the second-sound velocity with increasing temperature. However, for the case of NaF where experimental data are available, it is apparent that the temperature dependence due to the nonlinearity of the phonon spectrum is not sufficient to describe the experimental findings. The solution of Eq. (15) predicts a variation of the second-sound velocity from c_t to the $c_{II}(1+2r)^{-1/2}$ as the temperature increases and the system gradually moves from a purely ballistic regime into a hydrodynamic one. This agrees qualitatively and quantitatively well with the temperature dependence of this velocity found experimentally. A detailed numerical analysis of this will be published separately.

PHYSICAL REVIEW B VOLUME 5, NUMBER 8 15 APRIL 1972

Paraelectric Resonance of Ag^+ in RbCl†

Frank Bridges
University of California, San Diego, California 92037
and University of California, Santa Cruz, California 95060*

(Received 12 October 1971)

The paraelectric resonance (PER) of Ag^+ in RbCl for frequencies 7.3–36 GHz is reported. Assuming nearest-neighbor tunneling is dominant, the data are in agreement with the previously reported ⟨111⟩ orientation, and the observed dipole moment (uncorrected for local field) is 4.6 ± 0.1 D. Assuming a Lorentz local-field correction, this result can be interpreted as a charge e displaced approximately 0.5 Å along a ⟨111⟩ direction. The distortion of the PER line as a result of a large linewidth is discussed using a simple model, and the observed line shape at low frequencies is explained. An upper limit to the zero-field splitting is found to be 3.0 GHz.

I. INTRODUCTION

In recent years a number of investigators have studied paraelectric centers in alkali halides using paraelectric resonance (PER).[1–14] Of the centers studied so far using this technique most have been diatomic centers with a permanent electric dipole such as OH^- and CN^- in alkali halide hosts. Only one paraelectric system (Li^+ in KCl) in which the electric dipole is formed by an ion sitting off-center in the crystal has been studied in detail by PER.[4,5,10,12,14] We now report the investigation of another off-center system—Ag^+ in RbCl. A preliminary discussion of the results has been given previously.[15]

The system RbCl:Ag^+ has received considerable attention of late. Dreybrodt and Fussgaenger[16] observed a temperature dependence of the dipole oscillator strength and explained it on the basis of the Ag^+ displaced along ⟨111⟩ directions. Electrocaloric measurements of Kapphan and Lüty[17] indicated that the cation is oriented along ⟨111⟩ directions, forming an electric dipole moment with a magnitude of 4.0 ± 0.4 D (uncorrected for local field). Recent infrared studies[18] suggest that the off-center cation is oriented along ⟨110⟩ directions in the crystal and has a very small dipole moment. The present results generally agree with those of Kapphan and Lüty and the discrepancies between infrared studies and other measurements

are still unexplained.

The effects of linewidths in PER have been treated phenomenologically. Using a simple model, the distortion of the observed derivative signal, at low microwave frequencies where the Q of the line is ≤ 1, can be easily explained. The analysis shows that if the center of the line is taken as the zero crossing, the position of the resonance in electric field becomes nonlinear with microwave frequency in a manner suggestive of zero-field splitting effects. Thus, for low-Q lines, the center of the line is *not* at the zero crossing. We will, however, continue to use the zero crossing since it is an easily obtained experimental parameter.

The organization of the paper is as follows: The apparatus is described in Sec. II, followed by a presentation of the data in Sec. III; the interpretation of the results is given in Sec. IV and a summary of the conclusions is given in Sec. V.

II. METHOD AND APPARATUS

The measurements were taken on reflection spectrometers at the X band between 7.3 and 11.5 GHz and at the K_a band between 27 and 36 GHz. For most measurements, the power reflected from the cavity was observed using a 10-dB directional coupler as in Fig. 1. Although less sensitive than spectrometers which incorporate matched magic tees, these spectrometers operated over the entire waveguide band—a necessity for these experiments. A few measurements were also taken using matched magic tees with center frequencies of 9.2, 28.5, and 35 GHz. At the K_a band, two OKI klystrons were used—one covered the range 27–32 GHz and the other the range 32–36 GHz. At the X band, Varian V-58 klystrons were used. Several used klystrons were adjusted beyond their normal limits to give a total available range of 7.2–12 GHz.

At each frequency, the klystron was frequency locked to the microwave cavity using lock-in techniques. The error signal was applied to the klystron repeller using an electrooptical device which had dc response but allowed the output to float up to 5 kV. A G. E. SSL-5 photodiode and a G. E. L14A502 phototransistor were used. A similar electrooptical device has been described by Falick and Myers.[19]

A multimode cavity[20] was used for most of the measurements. The samples were lightly held against the wall (using a beryllium-copper spring) in such a manner that the dc and microwave electric fields were parallel. The stress applied to the 2-cm^2-size sample by the beryllium-copper spring was negligible as evidenced by no change in the paraelectric resonance signal (shape or position) when the spring was tightened slightly or when it was so loose that the sample was free to slide. (The latter case was very noisy.) A variation of the electrical contacts—from evaporated gold electrodes on the sample to holding the sample between metal plates via the beryllium-copper spring—also gave no change in the signal.

Standard lock-in techniques were used for detection. The electric field was modulated at frequencies between 0.04 and 4 kHz, and a PAR HR-8 lock-in detector was used to observe the derivative of the absorption signal.

The crystals were prepared from three boules grown at the Crystal Growing Facility at the University of Utah with Ag^+ concentrations of approximately 2–4, 20–40, and 100–200 ppm. The relative concentrations of Ag^+ were determined from the height of the absorption peak at 200 mμ.[16] Samples were oriented using an x-ray diffractometer and then cut using a string saw with water. Samples were oriented within $\frac{1}{2}°$ from the ⟨100⟩, ⟨111⟩ and ⟨110⟩ directions. After cutting, the orientation of the slice was checked and the sample then lapped using a small amount of water and methanol on a stretched linen cloth. Sample thickness ranged from 0.7 to 2 mm and were measured to 1%. A few samples which were mechanically polished gave slightly larger (<10% change) linewidths than the water-lapped samples.

The samples were fairly delicate and could be easily strained. The narrowest lines (<30% narrower) were obtained on samples which were very carefully handled using a vacuum holder (a device consisting of a soft plastic tube which could be partially evacuated when the open end of the tube was placed on the sample). Invariably, if the sample was removed and then remounted in the microwave cavity and rerun, the linewidth would be slightly larger. With the multimode cavity used in these experiments, the same cavity could be used between 7.3 and 36 GHz, and thus measurements could be taken over this frequency range on the *same* sample without reloading it.

Two different heat treatments were tried. First a quenching technique was tried to disperse any

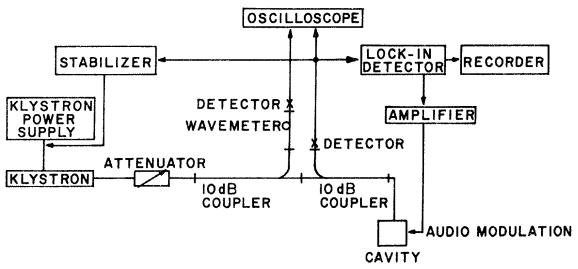

FIG. 1. Block diagram of the spectrometer for use across a waveguide band. For some measurements, the directional coupler was replaced by a magic tee.

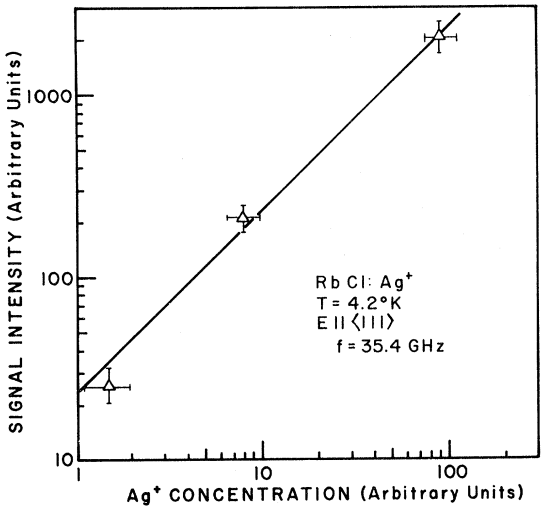

FIG. 2. Integrated intensity of the absorption line as a function of the Ag^+ concentration in RbCl. The graph shows that the integrated intensity is proportional to the number of centers in the sample.

clumping of silver impurities that may have occurred. The sample was heated to within 50 °C of its melting point in a RbCl crucible (argon atmosphere) and then rapidly cooled to room temperature. This procedure always gave broader lines, presumably produced by strains.

Secondly we tried annealing the samples to remove strains. The samples were held within 50 °C of melting for 1 h in a RbCl crucible in argon gas and then cooled slowly for 10 h to room temperature. Annealing of carefully made samples gave a negligible decrease in the linewidth of the observed signals (< 10%). This technique, when applied to samples previously quenched, narrowed the observed lines to their original value (within 5%).

III. EXPERIMENTAL RESULTS

Paraelectric resonance absorption of Ag^+ in RbCl was observed as a function of Ag^+ concentration, of temperature between 1.4 and 4.2 °K, of electric field orientation relative to the crystal axes, and of frequency between 7.3 and 36 GHz. In Fig. 2 the integrated intensity of the observed line for the applied field along a ⟨111⟩ direction and a frequency $\nu = 35.4$ GHz is plotted as a function of the Ag^+ concentration in the crystal. The data show that the observed strength of the resonance is proportional to the Ag^+ concentration and therefore is strong evidence that the observed signal is produced by Ag^+ in RbCl. No signals were observed in pure RbCl.

Typical experimental data of the derivative of the absorption curve is shown in Figs. 3 and 4 for frequencies 7.3–11 GHz and 27–36 GHz, respectively, for the electric field E parallel to a ⟨111⟩ axis. At the higher frequencies (27–36 GHz) the line is nearly symmetric, the position of the resonance (zero crossing) is proportional to the frequency, and the linewidth is constant. The data indicate that in the 27–36-GHz range the system is in the high-electric-field limit. As the frequency is lowered the observed signal becomes distorted—the negative part of the signal being much larger than the positive part. Moreover, the zero crossing is no longer proportional to the microwave frequency. This may be seen more clearly in Fig. 5 where the position of the resonance (taken as the zero crossing) is plotted as a function of frequency. This deviation from linearity is suggestive of a zero-field splitting effect but, as will be pointed out shortly, is caused by the breadth of the line.

At the lower microwave frequencies where the line was badly distorted, we were concerned whether or not we were observing pure absorption or a mixture of absorption and dispersion. To check this possibility, a phosphorus-doped silicon sample was also placed in the cavity and the paramagnetic signal observed simultaneously using a second lock-in detector. The paramagnetic signal

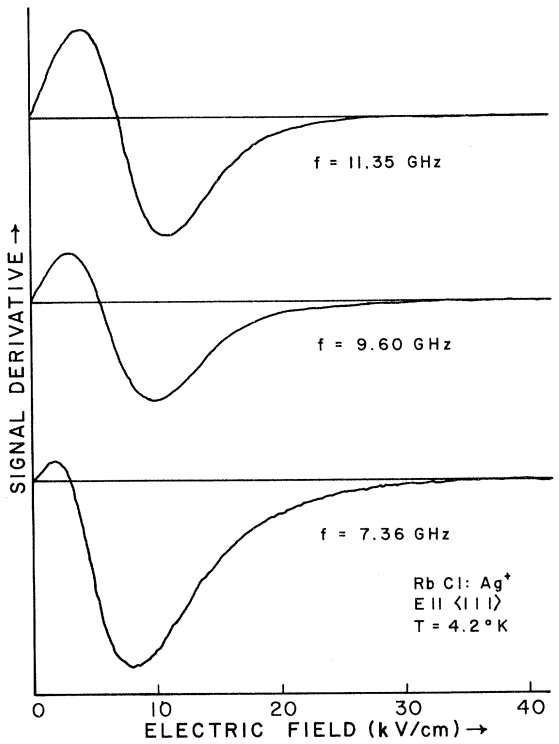

FIG. 3. Derivative signal at 7.36, 9.60, and 11.35 GHz for a ⟨111⟩ electric field. The distortion of the observed line and the rapid shift of the zero-crossing position to lower fields, when the frequency is lowered, are easily seen. This effect is attributed to the large linewidth.

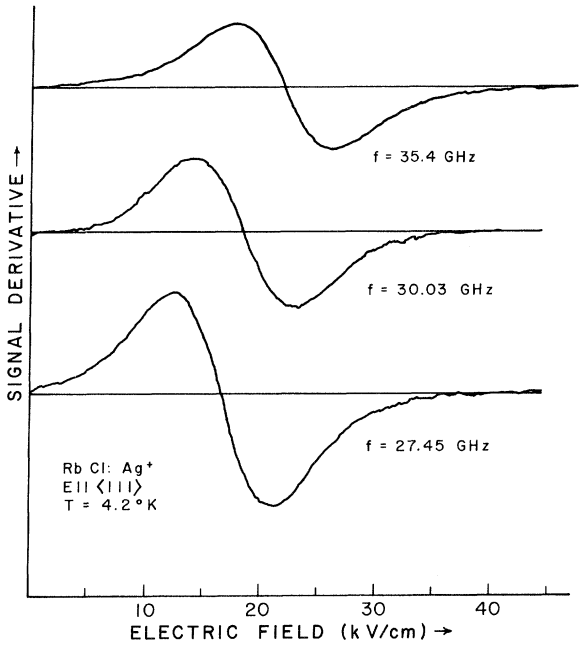

FIG. 4. Derivative signal at 27.45, 30.03 and 35.4 GHz for a ⟨111⟩ electric field. The line is very nearly symmetric, the linewidth is independent of frequency, and the zero crossing varies linearly with the electric field.

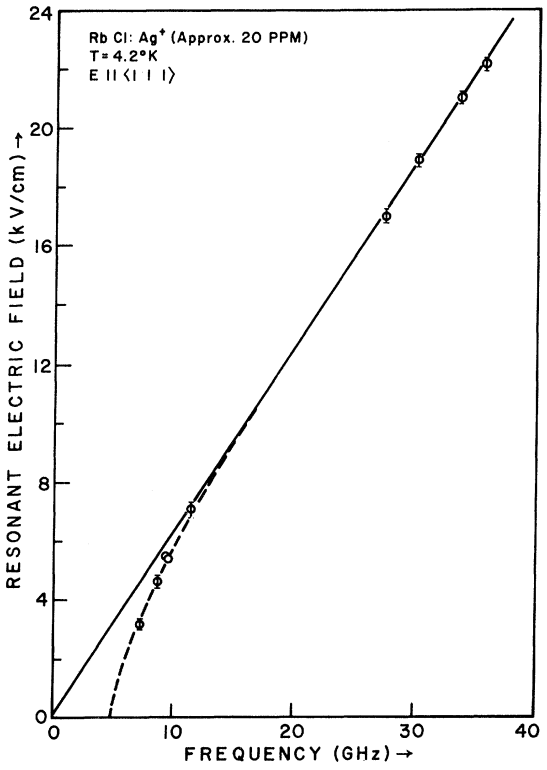

FIG. 5. Position in electric field of the zero crossing of the derivative signal as a function of the microwave frequency for ⟨111⟩ electric field. All measurements except the 7.3-GHz data were taken on the *same* sample. The deviation from linearity at low frequencies is a result of the large linewidth. The dotted line shows the effect of a zero-field splitting of 5 GHz when the effects of the linewidth are neglected.

was symmetric at all values of the electric field on the paraelectric sample, indicating that we were observing pure absorption.

Next let us consider the position of the center of the line, at *constant frequency*, as a function of the electric field orientation relative to the crystal axes in the high-electric-field limit. In Fig. 6 the resonance at 35.5 GHz is shown for the electric field along the ⟨100⟩, ⟨110⟩, and ⟨111⟩ axes. We define the field at which the zero crossing occurs for an orientation ⟨*ijk*⟩ as E_{ijk}. Then the observed ratios relative to the ⟨100⟩ orientation are

$$E_{111}/E_{100} = 1.71 \pm 0.05, \quad E_{110}/E_{100} = 1.39 \pm 0.05 .$$

Since as indicated earlier, we are in the high-field limit, these ratios should be independent of frequency. Experimentally the same ratios were observed at several frequencies between 27 and 36 GHz.

Measurements taken as a function of temperature give a temperature-independent linewidth of the PER signal. However, a strong temperature dependence was observed in the saturation of the system at $\nu = 9.6$ GHz. Below about 2 °K the system could be saturated fairly easily. Between 2 and 4.2 °K the ability to saturate the system with the available microwave power (50 mW) decreased

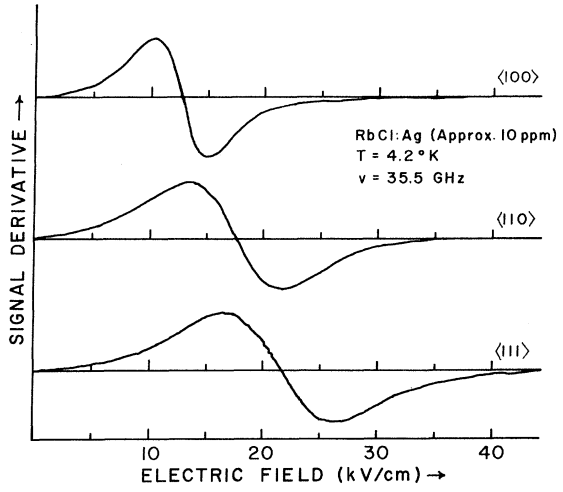

FIG. 6. Derivative signal at 35 GHz for the electric field parallel to the ⟨100⟩, ⟨110⟩, and ⟨111⟩ directions. The figure shows the dependence of the zero crossing on crystal orientation.

rapidly, and the system could not be saturated at 4.2 °K.

IV. INTERPRETATION

A. Model Hamiltonians

When Ag^+ is introduced into the RbCl host lattice, two positions of the ion are possible—one in which Ag^+ forms an interstitial impurity that is eventually frozen in position at low temperatures, and one in which the Ag^+ substitutionally replaces the Rb^+ ion. Since experimentally Ag^+ in RbCl forms an electric dipole that readily reorientates at low temperatures, the interstitial position is ruled out and it is assumed that Ag^+ replaces Rb^+ substitutionally. To produce an electric dipole an additional requirement must be imposed—the Ag^+ must not occupy a site of symmetry but must sit off-center along one of a set of symmetry directions in the crystal.[16,17] Reorientation between equivalent directions in the crystal is possible via a tunneling model. This model is a good approximation as long as the tunneling parameters are small as is the case in RbCl: Ag^+.

In this model it is assumed that a multiwell potential restricts the orientation of the dipoles to lie along one of the symmetry directions in the crystal. For octahedral symmetry the three most likely potentials are the XY_6 with 6 equivalent orientations along ⟨100⟩ directions, the XY_8 with 8 equivalent orientations along ⟨111⟩, and the XY_{12} with 12 equivalent orientations along ⟨110⟩ directions. Following Gomez *et al.*,[21] we define tunneling parameters η, μ, ν, σ to be the crystal-field matrix elements for tunneling between nearest-neighbor potential minima, next-nearest-neighbor potential minima, etc. Using Fig. 7, the matrix elements of the crystal-field Hamiltonian $\mathcal{H}_c$ are defined as follows:

XY_6 systems—two parameters:

$$\eta(90°) = \langle\alpha|\mathcal{H}_c|\gamma\rangle = \langle\alpha|\mathcal{H}_c|\epsilon\rangle \cdots ,$$

$$\mu(180°) = \langle\alpha|\mathcal{H}_c|\beta\rangle = \langle\gamma|\mathcal{H}_c|\delta\rangle \cdots ;$$

XY_8 systems—three parameters:

$$\eta(70.5°) = \langle 1|\mathcal{H}_c|6\rangle = \langle 1|\mathcal{H}_c|3\rangle \cdots ,$$

$$\mu(109.5°) = \langle 1|\mathcal{H}_c|4\rangle = \langle 1|\mathcal{H}_c|5\rangle \cdots ,$$

$$\nu(180°) = \langle 1|\mathcal{H}_c|2\rangle \cdots ;$$

XY_{12} systems—four parameters:

$$\eta(60°) = \langle a|\mathcal{H}_c|g\rangle \cdots ,$$

$$\mu(90°) = \langle a|\mathcal{H}_c|f\rangle \cdots ,$$

$$\nu(120°) = \langle a|\mathcal{H}_c|h\rangle \cdots ,$$

$$\sigma(180°) = \langle a|\mathcal{H}_c|b\rangle \cdots .$$

The splittings of the energy levels (called the zero-field splitting parameters) at $E = 0$ are determined by the tunneling parameters.

When the effects of an applied electric field are included, an additional term $\mathcal{H}_{\text{dipole}} = \vec{P}_\mu \cdot \vec{E}$ must be included to give

$$\mathcal{H} = \mathcal{H}_{\text{crystal}} + \mathcal{H}_{\text{dipole}} ,$$

where $\vec{P}_\mu$ is the apparent dipole moment, uncorrected for local-field effects, and $\vec{E}$ is the external electric field.

Several investigators[21-24] have obtained the energy levels as a function of electric field for various choices of dipole orientations and values of the tunneling parameters. It is useful to consider the results in the limits of high and low electric fields. For low electric fields ($\vec{P}_\mu \cdot \vec{E}$ < tunneling parameter) the energy levels are nonlinear in electric field and in many cases approach the zero-field values quadratically. In principle if one observes paraelectric resonance at several frequencies just above the zero-field splitting value, one should be able to infer the value of the zero-field splitting. This limit is not applicable to the RbCl: Ag^+ system since for the frequencies ω available, $\hbar\omega \gg$ zero-field splitting.

In the high-field limit a first approximation is to neglect the effects of the zero-field splitting parameters in the energy levels and only introduce the tunneling parameters to determine which transitions are allowed. One may then ask the question: How does the position of the resonance line vary in electric field as the orientation of the field is changed? For a constant microwave frequency, the ratios of the resonance position for ⟨111⟩ and ⟨110⟩ directions of field relative to the ⟨100⟩ direction are given in Table I using the definitions

$$\alpha = E_{111}/E_{100} , \quad \beta = E_{110}/E_{100} .$$

There are of course many other possible values of the tunneling parameters that could be consid-

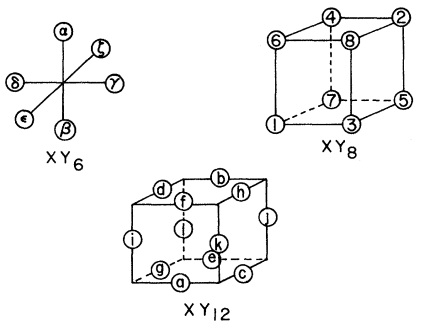

FIG. 7. Orientations of the dipoles for the three systems. The crystal-field matrix elements are defined using this labeling.

TABLE I. Ratios of the positions of allowed PER transitions at a constant microwave frequency for different orientations of the electric field. The notation is that of Gomez *et al.* (Ref. 21). The parameters α and β are defined by $\alpha = E_{111}/E_{100}$, $\beta = E_{110}/E_{100}$.

	XY_6	XY_8	XY_{12}
	$\mu = 0$	$\mu, \nu = 0$	$\mu, \nu, \sigma = 0$
$\eta \neq 0$	$\alpha = \frac{1}{2}\sqrt{3}$; $\beta = \sqrt{2}, \frac{1}{2}\sqrt{2}$	$\alpha = \sqrt{3}$; $\beta = \sqrt{2}$	$\alpha = \frac{1}{2}\sqrt{3}$; $\beta = \sqrt{2}, \frac{1}{2}\sqrt{2}$
	$\eta = 0$	$\eta, \nu = 0$	$\eta, \nu, \sigma = 0$
$\mu \neq 0$	$\alpha = \sqrt{3}$; $\beta = \sqrt{2}$	$\alpha = \frac{1}{2}\sqrt{3}$; $\beta = \sqrt{2}, \frac{1}{2}\sqrt{2}$	$\alpha = \sqrt{3}$; $\beta = \sqrt{2}$
		$\eta, \mu = 0$	$\eta, \nu, \sigma = 0$
$\nu \neq 0$		$\alpha = \frac{1}{3}\sqrt{3}, \sqrt{3}$; $\beta = \frac{1}{2}\sqrt{2}$	Many lines
			$\eta, \mu, \sigma = 0$
$\sigma \neq 0$			$\alpha = \frac{1}{2}\sqrt{3}$; $\beta = \sqrt{2}, \frac{1}{2}\sqrt{2}$

ered. When one of the tunneling parameters dominates, the ratios of Table I are expected; if two or more parameters are comparable, the ratios will be different from those listed.

It is interesting to note that the same ratios α and β can be obtained for more than one system. In particular, $\alpha = \sqrt{3}$, $\beta = \sqrt{2}$ is possible for the XY_6 system with $\eta = 0$, $\mu \neq 0$ (180° tunneling), for the XY_8 system with $\eta \neq 0$, $\mu, \nu = 0$ (edge tunneling—70.5°), and the XY_{12} system with $\mu \neq 0$, $\eta, \nu, \sigma = 0$ (face tunneling—90°). In fact for these choices of tunneling parameters the ratio E_{ijk}/E_{100} will be the same for all three systems for any orientation of field. Therefore some assumptions must be made about the tunneling parameters before the orientation data can be interpreted.

B. Interpretation of Data

The temperature dependence of the resonance gives two results. First the independence of the linewidth with temperature indicates that the phonon contribution to the broadening is small. This is consistent with a system broadened by either internal strains or internal electric fields. Secondly, the rapid decrease in the ability to saturate the resonance, which occurs just above 2 °K indicates that the dipole-lattice relaxation rate $1/T_1$ is changing very quickly with temperature. The crossover point between a slow temperature dependence and a fast temperature dependence occurs around 2 °K and may be the crossover point from $1/T_1 \propto T$ to a very rapid temperature dependence which may not have a simple analytical solution.[25–29] Using the power level at which the normalized signal intensity drops to $\frac{1}{2}$ (with no saturation, the normalized signal should be 1), one can obtain a rough estimate of the temperature dependence. The preliminary data indicates that between 2.3 and 3 °K the dependence could be described by $1/T_1 \propto T^n$ where $n \simeq 5$. Further measurements will be made to understand the relaxation in more detail.

In Fig. 5, the position of the zero crossing of the derivative curve deviates from linearity with frequency below 10 GHz. This is the expected response when the microwave energy approaches the zero-field splitting energy. If one assumes that the orientation of the dipoles is ⟨111⟩ with $\eta \gg \mu, \sigma$ and a zero-field splitting of 5 GHz, then the data agree fairly well with the calculated curve as shown by the dotted line in Fig. 5. However, the effects of the linewidth are neglected in such an interpretation.

Instead, let us make the following assumptions: (i) The zero-field splitting is small compared to the microwave energies available; (ii) at 35.4 GHz there is negligible overlap of the lines at plus and minus E fields and thus the observed signal (35.4 GHz) may be used to give the shape function of the line; and (iii) for simplicity, assume that the linewidth is produced by a distribution of electric fields in the sample. In this model the linewidth remains constant as the frequency is changed as is experimentally observed between 27 and 36 GHz. The absorption of energy must be symmetric in electric field E, and therefore the derivative must be antisymmetric. Let $A(f, E)$ be the absorption signal at a frequency f and $A'(f, E)$ the derivative with respect to E. Then

$$A(f, E) = A(f, -E), \quad A'(f, E) = -A'(f, -E) .$$

As the microwave frequency is lowered the tails of the resonance for positive and negative E fields will start to overlap at low electric fields, thereby distorting the observed resonance line.

We will define $G'(\epsilon)$ as the derivative shape function obtained from the data at $f_0 = 35.4$ GHz with a zero crossing at $E = E_0$. $G'(\epsilon) = 0$ at $\epsilon = 0$. Then we can calculate the expected line shape as a function of E at lower microwave frequencies by shifting the high-field line to lower fields by the same fractional change as the decrease in the frequency,

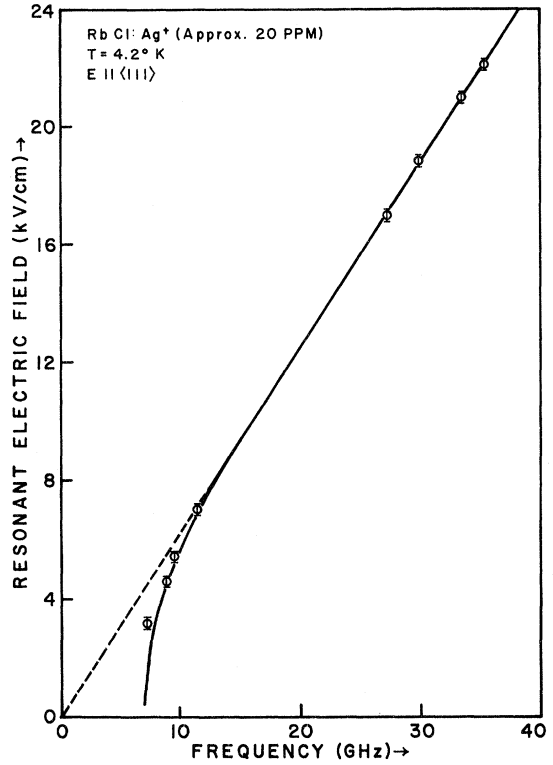

FIG. 8. Position in electric field of the zero crossing of the derivative signal as a function of the microwave frequency for ⟨111⟩ electric fields. All data except the 7.3 GHz were taken on the *same* sample in the same cavity. The solid line is the calculated position of the zero crossing using the 35.4-GHz data.

i.e.,

$$A'(f,E)=G'(E-hf/P_\mu)-G'(-E-hf/P_\mu)\ ,$$

where $G'(\epsilon)=0$ for $\epsilon\leq -E_0$,

$$f=(1-\alpha/E_0)f_0\ ,$$

and the actual center of the line is at

$$E_0'=E_0-\alpha\ .$$

The calculated zero crossings (not line centers) are compared in Fig. 8 with the data taken on the *same* sample at several frequencies (without handling the sample). The good agreement is even more striking when one compares the observed and calculated line shapes as shown in Fig. 9 for 8.8 GHz. To check the effect of changes in the linewidth, a second calculation was made with the 35.4-GHz data broadened by 10%. The calculated line for 8.8 GHz then showed a much larger distortion and the zero crossing moved down in field by 20%. Therefore we conclude that the observed distortion and shift of the zero crossing of the observed resonance at low frequencies must be a result of the large linewidth and not the effect of the zero-field splitting. Moreover if the zero-field splitting is $\leq \frac{1}{4}$ (linewidth energy), its effect will probably not be observed (less than a 4% effect). We place an upper limit of 3.0 GHz on the zero-field splitting.

Similar linewidth-dependent zero crossings of paraelectric resonance lines have been observed in other systems—notably KCl:OH^- where the zero crossing was observed to move to a higher electric field when the linewidth was decreased.[8] For this system, the linewidth energy is of the order of the microwave energy used, and an analysis which includes the distortion near zero electric field which results from the overlap of the tails of resonances at positive and negative electric fields should explain these observations in KCl:OH^-.

Next, consider the orientation data. The experimental values for α and β are very close to $\sqrt{3}$ and $\sqrt{2}$, and therefore we have one of three possibilities—an XY_6 system, with $\mu \gg \eta$, an XY_8 system with $\eta \gg \mu$, ν or XY_{12} with $\mu \gg \eta, \nu, \sigma$. It is probably reasonable to assume that 180° tunneling does not dominate over 90° tunneling for the XY_6 system, and thus we can eliminate this system.

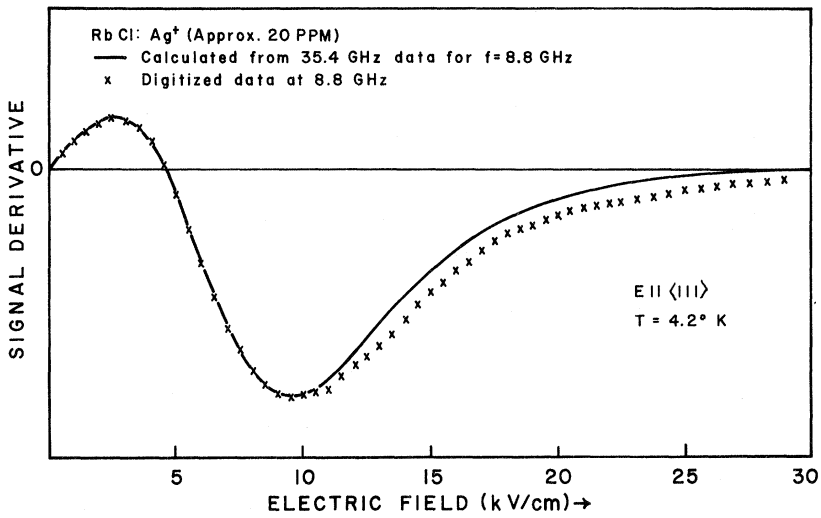

FIG. 9. Line shape at 8.8 GHz. The figure shows good agreement between the line calculated using the 35.4-GHz data and the 8.8-GHz data taken on the *same* sample. The calculation was normalized to give the same peak-to-peak height.

For the XY_8 system $\eta \gg \mu, \nu$ (nearest-neighbor tunneling) is a reasonable assumption, but for the XY_{12} system the situation is not obvious. It is easy to conceive of a potential for which the tunneling parameter μ for second-nearest-neighbor tunneling is important—for example, a potential with a saddle point in the ⟨100⟩ directions. However, for such a potential, nearest-neighbor tunneling could also proceed via the ⟨100⟩ directions and thus both η, μ should be important. To have $\mu \gg \eta$ places strong restrictions on the potential, and we therefore suggest that the observed ratios probably indicate that the dipole orientation is ⟨111⟩ in agreement with Kapphan and Lüty and Dreybrodt and Fussgaenger, but not with Kirby *et al.* If other experiments definitely resolve the orientation of the dipole, then the PER orientation data will indicate which tunneling parameters are dominant.

Finally, the electric dipole moment P_μ (uncorrected for local fields) may be obtained from the high-field slope of the line position vs frequency data (Fig. 5). Assuming a ⟨111⟩ orientation for the dipoles, then[30]

$$P_\mu = 4.6 \pm 0.1 \text{ D} .$$

This agrees fairly well with the value 4.0 ± 0.4 D obtained by Lüty *et al.*, but disagrees strongly with the infrared data of Kirby *et al.*, for which P_μ is very small.

If one attempts to correct for local-field effects using the Lorentz local field, a corrected dipole moment of 2.03 D is obtained. Interpreting this dipole as a charge e displaced a distance r along a ⟨111⟩ direction gives a value for r of 0.43 Å. This agrees well with the theoretical value of 0.54 Å calculated by Wilson *et al.*[31] and is less than a factor 2 larger than the value obtained by Dreybrodt and Fussgaenger.[16] Considering that the Lorentz local-field correction is only an approximation for permanent dipoles, the agreement is reasonable.

The disagreement of the infrared data with PER and electrocaloric data, along with recent data of Hanson,[32] and the fact that Lüty's data did not fit the ⟨111⟩ orientation exactly, point out that the RbCl:Ag^+ is probably not a simple system. Ag^+ may for example form more than one type of center in RbCl.[18] The variations in the observations would then be attributed to different experiments having different relative sensitivities for each type of center.

V. CONCLUSIONS

The observed paraelectric resonance is attributed to off-center Ag^+ in the RbCl host. The orientation data agree with the ⟨111⟩ orientation obtained by Kapphan and Lüty, and Dreybrodt and Fussgaenger,[16] if one assumes nearest-neighbor tunneling is dominant. However, if one assumed that one of the other tunneling parameters is dominant, then the data agree with a ⟨110⟩ orientation if $\mu \gg \eta, \nu, \sigma$ (face tunneling) or a ⟨100⟩ if $\mu \gg \eta$ (180° tunneling).

Assuming a ⟨111⟩ orientation, an electric dipole moment of 4.6 ± 0.1 D is obtained. Using a Lorentz local-field correction, this result may be interpreted as a charge e displaced approximately 0.43 Å along the ⟨111⟩ direction, in fair agreement with the theoretical value.[31]

The shift of the zero crossing and the distortion of the PER line at low frequencies has been explained assuming that the tails of resonance lines for positive and negative E fields, overlap at $E = 0$. Assuming that the broadening may be represented by a distribution of electric fields in the sample, and that the zero-field splitting is very small, the line shape calculated for low frequencies (8.8 GHz) using the high-frequency data (35.4 GHz) agrees very well with the low-frequency experiments on the *same* sample. This simple analysis shows that if the linewidth energy $\geq 4X$ (zero-field splitting), the effects of the zero-field splitting will be masked (less than a 4% effect). After correcting the data for linewidth effects an upper-limit estimate for the zero-field splitting was found to be 3 GHz.

The saturation data indicated that the temperature dependence of the relaxation rate changed rapidly around 2 °K. More work is necessary to check this result.

The disagreement between infrared studies and other measurements is still unexplained. This might be a result of Ag^+ forming several types of PER centers with the possibility that different experiments are sensitive to different impurities.

ACKNOWLEDGMENTS

I wish to thank G. Feher, H. Shore, and F. Lüty for many useful discussions. I also wish to thank R. Hanson for informing me of his results prior to publication.

†Work sponsored in part by the National Science Foundation.

*Present address.

[1]W. E. Bron and R. W. Dreyfus, Phys. Rev. Letters 16, 165 (1966); Phys. Rev. 163, 304 (1967).

[2]G. Feher, I. Shepherd, and H. Shore, Phys. Rev. Letters 16, 500 (1966).

[3]L. E. Shearer and T. L. Estle, Solid State Commun. 4, 639 (1966).

[4]G. Höcherl, D. Blumenstock and H. Wolf, Phys. Letters 24A, 511 (1966).

[5]G. Höcherl and H. Wolf, Phys. Letters 27A, 133 (1968).

[6]T. L. Estle, Phys. Rev. 176, 1056 (1968).

[7]R. W. Dreyfus, J. Phys. Chem. Solids 29, 1941 (1968).

[8]R. W. Dreyfus, Solid State Commun. 7, 827 (1969).

[9]R. S. Scott and W. H. Flygare, Phys. Rev. 182, 445 (1969).

[10]R. A. Herendeen and R. H. Silsbee, Phys. Rev. 188,

645 (1969).
[11]R. W. Timme, B. Dischler, and T. L. Estle, Phys. Rev. B 1, 1610 (1970).
[12]A. V. Frantessan, O. F. Dudnik, and V. B. Krauchenko, Fiz. Tverd. Tela 12, 160 (1970) [Sov. Phys. Solid State 12, 126 (1970)].
[13]D. Blumenstock, R. Osswald, and H. C. Wolf, Z. Physik 231, 333 (1970).
[14]W. G. Van Holle, J. H. S. Wang, R. S. Scott, and W. H. Flygare, Solid State Commun. 8, 1363 (1970).
[15]F. Bridges, Bull. Am. Phys. Soc. 15, 787 (1970).
[16]W. Dreybrodt and K. Fussgaenger, Phys. Status Solidi 18, 133 (1966).
[17]S. Kapphan and F. Lüty, Solid State Commun. 6, 907 (1968).
[18]R. D. Kirby, A. E. Hughes, and A. J. Sievers, Phys. Rev. B 2, 481 (1970).
[19]A. M. Falick and R. J. Meyers, Rev. Sci. Instr. 40, 1349 (1969).
[20]F. Bridges (unpublished).
[21]M. Gomez, S. P. Bowen, and J. A. Krumhansl, Phys. Rev. 153, 1009 (1967).
[22]P. Sauer, O. Schirmer, and J. Schneider, Phys. Status Solidi 16, 79 (1965).
[23]H. B. Shore, Phys. Rev. 151, 570 (1966).
[24]M. E. Bauer and W. R. Salzman, Phys. Rev. 151, 710 (1966).
[25]J. A. Sussman, Physik Kondensierten Materie 2, 146 (1964).
[26]B. G. Dick, Phys. Status Solidi 29, 587 (1968).
[27]L. A. Vredevoe, Phys. Rev. 153, 312 (1968).
[28]B. G. Dick and D. Strauch, Phys. Rev. B 2, 2200 (1970).
[29]L. M. Sander and H. B. Shore, Phys. Rev. B 3, 1482 (1971).
[30]If the orientation is actually ⟨110⟩, an additional factor of $(\frac{2}{3})^{1/2}$ is required.
[31]W. Wilson, R. D. Hatcher, R. Smoluchowski, and G. J. Diennes, Phys. Rev. 161, 888 (1967); 184, 844 (1969).
[32]R. Hanson, J. Hollberg, and H. Shuman (private communication). Dielectric-constant and elastic measurements yield different apparent orientations of the electric and elastic dipoles.

PHYSICAL REVIEW B VOLUME 5, NUMBER 8 15 APRIL 1972

Transient Photoinjection of Holes from Amorphous Se into Poly(*N*-Vinyl Carbazole)

J. Mort
Research Laboratories, Xerox Corporation, Rochester, New York 14603
(Received 29 March 1971)

The transient photoinjection of holes from amorphous selenium into layers of poly(*N*-vinyl carbazole) (PVK) has been studied. A variety of techniques are described which lead to the conclusion that no barrier to injection need be invoked. The injection threshold observed in the Se:PVK structure using the xerographic condenser technique can be accounted for in terms of the achievement of space-charge-perturbed currents in the polymer dielectric. The steepness of the observed threshold arises from the field dependence of the drift mobility of holes in PVK.

I. INTRODUCTION

Regensburger[1] has recently described the sensitization of the dielectric poly(*N*-vinyl carbazole) (PVK) by overcoating with a thin layer of amorphous selenium as a sensitizer. The sensitization was studied using a xerographic condenser discharge technique and the results were interpreted as the injection of holes photogenerated in the amorphous Se into PVK. An abrupt drop in the gain of the system was observed on going to lower fields.

Several possibilities exist for the origin of what Regensburger termed a threshold field for carrier injection. These can be conveniently classified into two categories. One would be the presence of some type of "injection barrier" as suggested by Regensburger.[1] This could have its origin in a potential energy barrier due to the mismatch of electronic energy levels in the sensitizer and the dielectric, or it could result from macroscopic mechanical barrier at the interface between the sensitizer and the dielectric. The second category would arise, not because of any injection or interface limitation, but rather from bulk properties. Two outstanding possibilities in this class would be a range limitation in either the sensitizer (or the dielectric) or an absence (or at least reduction) of the field within the sensitizer due to permanent charge accumulation at the sensitizer-dielectric interface. As far as the bulk limitations are concerned, the range limitation can be eliminated in the amorphous Se: PVK system because of the independent knowledge of the ranges of Se[2] and PVK[3] from transient measurements.

The aim of this paper is to indicate from an investigation of transient photoconductivity in Se: PVK structures that a decrease in injection efficiency observed in the xerographic mode can arise from the trap-free space-charge-perturbed currents (TFSCPC) in PVK.